Mine Water Environ (2017) 36:78–86
DOI 10.1007/s10230-016-0405-5

TECHNICAL ARTICLE

# Hydrochemical Prediction of Mine Water Inrush at the Xinli Mine, China

**Guoqing Li[1] · Zhaoping Meng[2] · Xinqing Wang[1] · Jian Yang[3]**

Received: 16 November 2014 / Accepted: 4 June 2016 / Published online: 18 June 2016


**Abstract** Seawater poses a great threat to the Xinli Mine, an undersea gold mine in China. A hydrochemical method was used to assess the risk of sea water inrush into the mine. A detailed hydrochemical survey and sampling were carried out and the concentrations of conservative ions in the mine water were analyzed. Principal component analysis indicated that the potential water inrush channels were located in the hanging wall of the ore-controlling fault. A composite principal component was calculated from the $Na^{+}$, $Cl^{-}$, $Mg^{2+}$, $SO_4{}^{2-}$, and $K^{+}$ concentrations, which reflected the effects of potash feldspathization and cation exchange, to assess the risk of seawater inrush.

**Keywords** Hydrochemistry · Undersea mining · Water sources · Principal component analysis · Seepage channel

## Introduction

Water inrush in a mine is usually determined by three factors: the water source, aquifuge, and permeable channel(s). Examples of techniques used to assess the risk of a water inrush event in an underground coal mine include the water inrush coefficient, the vulnerable index, and lithological-structure methods (Meng et al. 2012; Wu et al. 2011; Xu and Wang 1991). Usually, groundwater inflow prediction in an underground mine is an engineering geology problem. Seepage channels are detected by drilling, geochemical, and geophysical methods, and then the channels are grouted.

However, there is very limited research on the hydrogeology of underwater excavations. The Xinli Mine is a modern undersea gold mine in Shandong Province, China (Sun et al. 2002). Seawater inrush there could cause many casualties and much economic loss. Because there are no karst collapse columns in this region, seawater can flow into the mine only through rock fractures. The hydraulic conductivity of rock fractures is generally controlled by fracture aperture and effective stress (Singhal and Gupta 2010; Zimmerman 2000; Zimmerman and Bodvarsson 1996). Underground excavation can induce significant rock movement, ground surface fissures, and even the collapse of mine shafts and roadways (Li et al. 2004; Ma et al. 2013; Zhao et al. 2012a, b, 2013). For example, at a metal mine in Gansu Province China, in situ high precision GPS measurements revealed that the maximum cumulative subsidence reached up to 1613 mm; as a result, many ground surface fissures occurred in the mine area (Zhao et al. 2012a, b). However, because the Xinli mine area is largely covered by seawater, we cannot perform GPS measurements and it is hard to detect seepage channels using routine drilling or geophysical methods. Thus, predicting and controlling seawater inflow has been very challenging.

Various factors influence groundwater quality and flow in coastal areas-such as seawater intrusion, deep brine water intrusion, return flow of agricultural irrigation, domestic and industrial wastewaters, ion exchange, evaporation, and over-extraction of groundwater-making it

**Electronic supplementary material** The online version of this article (doi:10.1007/s10230-016-0405-5) contains supplementary material, which is available to authorized users.

✉ Guoqing Li
ligq@cug.edu.cn

[1] Faculty of Earth Resources, China University of Geosciences, Wuhan 430074, China

[2] College of Geosciences and Surveying Engineering, China University of Mining and Technology, Beijing 100083, China

[3] China Coal Technology and Engineering Group, Xi'an Research Institute, Xi'an 710054, China

difficult to differentiate mine water sources from water quality data (Mondal et al. 2011; Moujabber et al. 2006; Salem et al. 2011; Seki et al. 1986). The aim of this study was to ascertain the mine water sources and to locate the potential seawater inrush seepage channels in the Xinli Mine. We used a hydrochemical approach. After studying the local geological settings, we carried out a detailed site survey and water sampling, and then we determined the concentrations of conservative ions. Subsequently, based on the hydrochemical analysis and reinforced by multivariate analysis, we identified water sources, water–rock interactions, and seepage channels and proposed an indicator to evaluate the risk of sea water inrush (Fig. 1).

## Materials and Methods

### Geological Setting

#### *Stratigraphy and Structure*

The Xinli goldmine, with a proven reserve of 30,000 kg of Au, is located in Laizhou City (Shandong Province) and is one of the largest goldmines in China. The NE-striking Sanshandao-Cangshang Fault, F1, is the ore-controlling fault for three mines (the Cangshang, Xinli and Sanshandao Mines) and extends into the Bohai Sea (Figs. 2, 3). All of the ore deposits are located in the footwall rock mass of F1 at these three mines. The local strata include the Mesoarchean Tangjiazhuang Group (Ar3t), the Neoarchean Jiaodong Group (Ar4j), Paleoproterozoic Jingshan Group (Pt1j), Feizishan Group (Pt1f), and Quaternary System (Q). The shear zone hosts the gold, which was deposited as a result of structural hydrothermal alteration. The mineralized alteration zone of the Xinli gold mine is 70–185 m wide and approximately 1000 m deep (maximum). The ore body being mined is only 10–30 m thick. The alteration zone comprises medium-to fine-grained metagabbro, monzogranite granite, cataclastic granite, beresitized granite, and beresitized catasclasite (supplemental Fig. 1). $F_1$ stretches for 1300 m to the NE, dipping SE at an angle of 45°–75°. The $F_1$ strikes averagely N62° E in the west and N38° E in the east and extends for above 600 m underwater. The fault $F_2$, exposed by five wellbores, is located in the northern sector of the Xinli mine area. It strikes N290° W and dips NE at an angle of 80°–90°.

#### *Hydrogeology*

The elevation of the mine entry ranges from 1.2 to 4.5 m above sea level, and decreases from the southeast to the northwest. The Wang River flows northeast of the mine area and a few fish ponds lie in the southeast. The Wang River flows into the sea only during July and August; it is dry the rest of the year. The overlying sea water in the northwest of the mine area is approximately 10 m deep. The Quaternary System is widely distributed in the area, with a thickness of 8–10 m. Above the ore-bearing strata, from bottom to top, the Quaternary seabed covers subclay, subsand, marine mud, silty clay, medium-fine sand, medium-coarse sand, and coarse gravel (Sun et al. 2002).

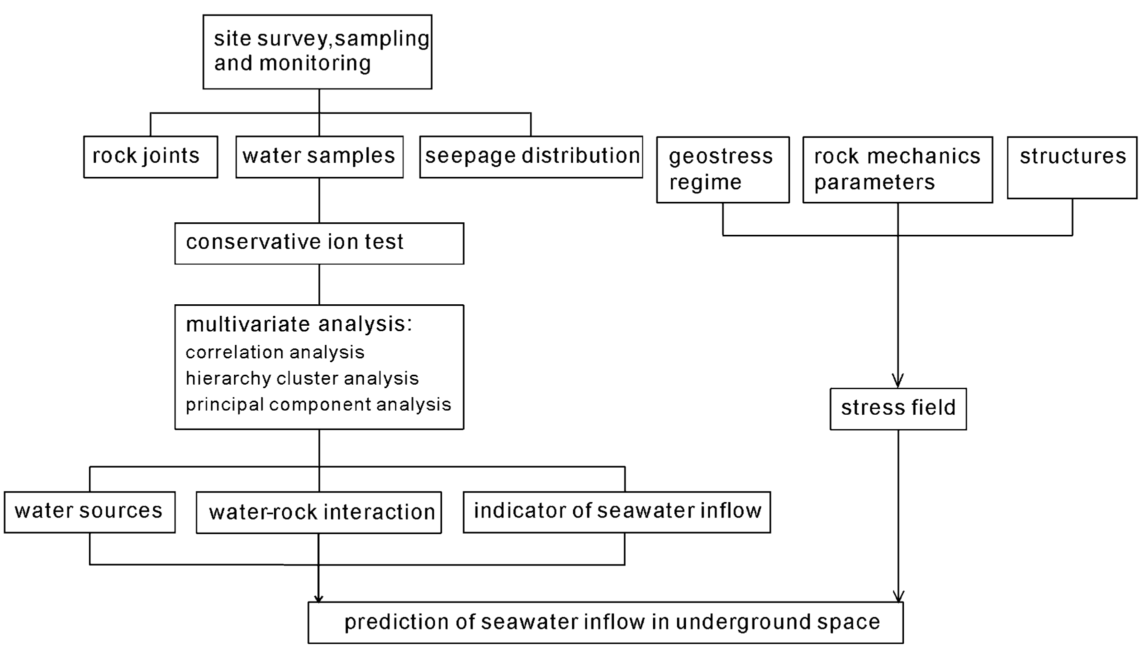


**Fig. 1** Workflow of seawater inflow prediction

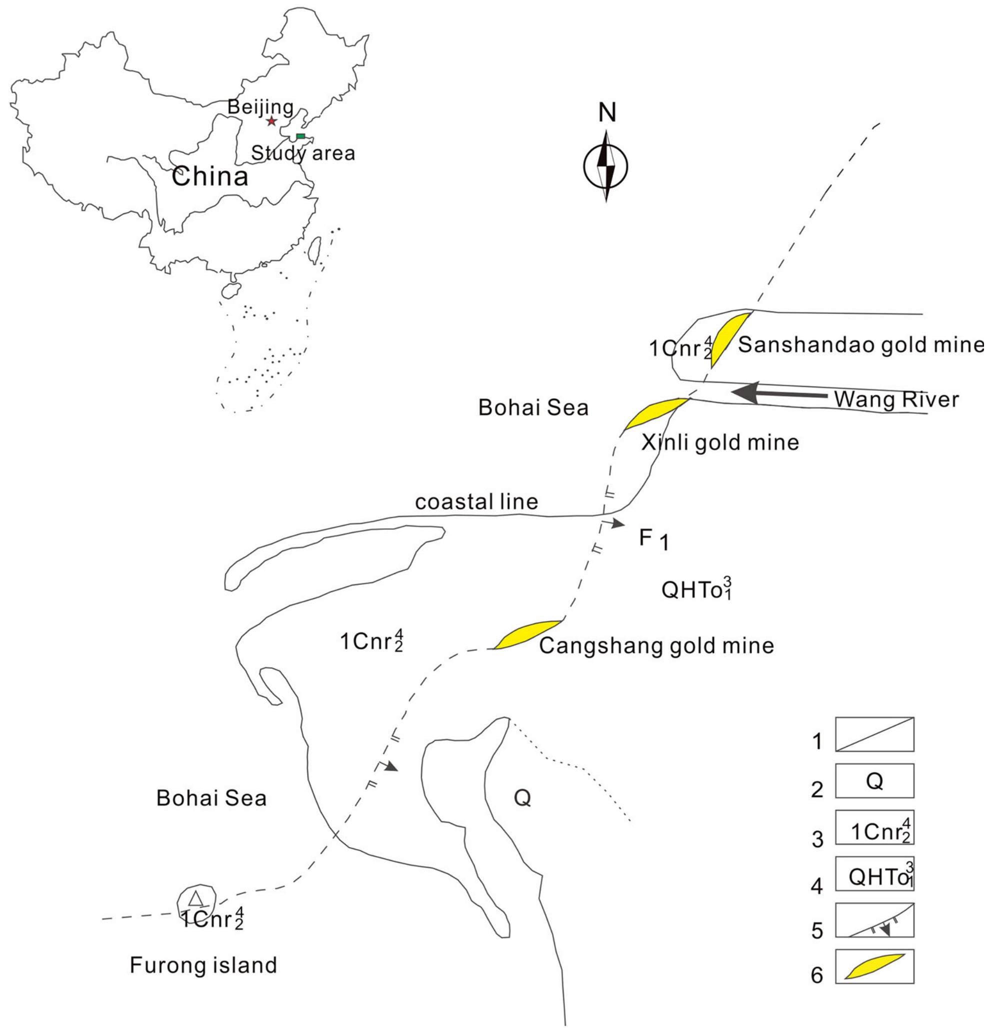


**Fig. 2** Regional geology of the study area: *1* Coastline, *2* Quaternary, *3* Cuizhao unit of the Linglong superunit, *4* the Luanjiazhan unit of Malianzhuang superunit, *5* Fault, *6* Gold mine

The Xinli gold mine operates using the state-of-the-art cemented upward-filling mining method. The fill material is mainly cement and tailings. The design drainage capacity of the underground sump is 5000 $m^3$/day. The mine water inflow is approximately 2000 $m^3$/day and largely comes from the −105 and −135 m sublevels near the mined out area in the northeast. Overall, the rock permeability coefficient is rather low. According to the packer permeability test, the permeability coefficient of the weathered rock below the Quaternary (at approximately the −75 m level) is $2.5 \times 10^{-7}$ m/s.

The possible sources of the mine water include the Bohai Sea, the Wang River, brine from in-rock fissures, and the Quaternary phreatic aquifer. The seawater is the greatest threat to safe production. Possible seepage channels into the mine pit include the F1 and F2 faults, rock joints, the weathered rock overburden, and the permeable Quaternary layers. There are fault gouges in both the F1 and F2 fault planes. The F1 gouge is rich in clay minerals and is approximately 0.05–0.1 m thick (supplemental Fig. 2). The F2 gouge is dark gray mud and is about 0.02–0.1 m thick. The bottom Quaternary layer, which is mainly composed of clay, silty clay, and marine mud, is impermeable and largely blocks contact with the pore water, seawater, and the fractured rock masses. However, this layer is variably 0.8–10 m thick and this high variability casts doubts over its impermeability (Li et al. 2012, 2014a, b; Liu et al. 2012; Zhao et al. 2012a, b).

## Site Survey and Sampling

To investigate the seepage of mine water into the mine, we carried out a detailed site survey in the −105 and −135 m sublevels. The accessible roadway in those sublevels is 1135.1 and 1336.0 m, respectively. We recorded all of the seepage points and collected typical water samples. To compare the hydrochemistry of the mine water with surface waters over the mine area, we also collected samples from the sea, ponds, drinking wells, precipitation, and the Wang River. Along the roadways, joints were measured using the

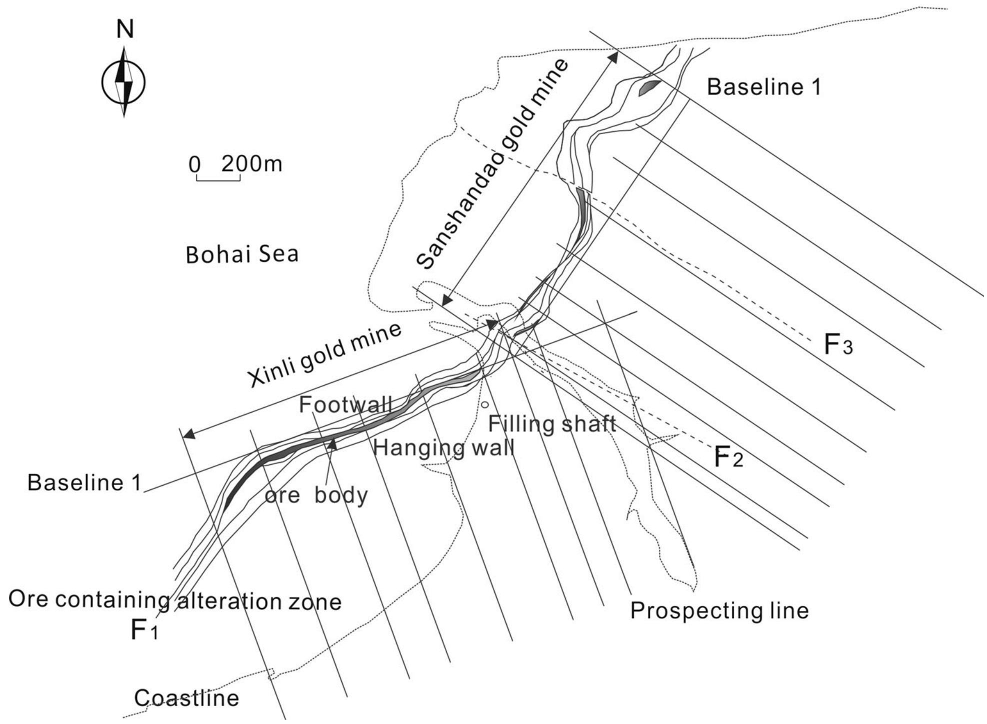


**Fig. 3** Geological sketch of the Sanshandao-Xinli fault

window method: a fixed frame of 1 m × 1 m was used to define the joint survey area every 10 m along one side of the roadway.

### Conservative Ion Test

Seawater has a very stable hydrochemistry. The conservative ions in the water samples were determined in the State Key Laboratory of Earthquake Dynamics (SKLED) Institute of Geology (part of the China Earthquake Administration), using the standard methods of the People's Republic of China: $Ca^{2+}$ and $Mg^{2+}$ were analyzed using the EDTA titration method (GB7477-87, GB7476-87); $K^+$ and $Na^+$ were analyzed by flame atomic absorption spectrometry (GB11904-89); $Cl^-$ was measured using the titration method; and $SO_4^{2-}$ was determined using the gravimetric method (GB 11899-89).

### Multivariate Statistics

If there are significant hydrochemical differences among possible water sources, the main water source can be identified by temperature, water quality, and water level. However, if the hydrogeology is very complex and the hydrochemical differences between the possible sources are minor, such as, for instance, at the Xinlin Mine, an indicating index can be determined using multivariate statistics to assess the potential source(s). We therefore performed correlation analysis, hierarchical clustering analysis (HCA), and principal component analysis (PCA). Due to the wide variation of ion concentrations, the Z-Score method was used to standardize the values of each variable (Eq. 1).

$$Z = (x - \mathrm{MEAN}(x))/\mathrm{STD}(x) \quad (1)$$

where Z is the Z-Score, x is the original value of a variable, MEAN(x) is the mean of all the values of a variable, and STD(x) is the standard variation of all the values of a variable, respectively.

HCA can effectively merge individual samples into homogeneous groups. However, one shortcoming of HCA is that it cannot express the correlations of each variable of all samples. For instance, $Cl^-$, mineralization, and electrical conductivity (EC) of water samples often show perfect pairwise linear correlations, so only one of these three variables was selected for multivariate statistics. The other shortcoming of HCA is that it cannot reveal water–rock interactions.

PCA is central to the study of multivariate data. PCA can reduce the dimensionality of a data set in which there are a number of interrelated variables, while retaining as much as possible of the variation present in the data set (Güler et al., 2012; Jolliffe 2002; Guo 2004; Kurchikov and Plavnik 2009). PCA transforms the original variables into a few new variables, which are called principal components (PCs). The PCs are orthonormal and can simplify the structure of the data set and sometimes reveal hidden information in the data set. The PCA includes the following successive steps: (1) compute the correlation matrix of the original variables; (2) calculate the eigenvalue and eigenvector of the correlation matrix; (3) analyze the contribution rate of the PCs; (4) determine the loadings of the original variables on the PCs; and (5) calculate the scores of the PCs. Based on the PCs of the data set, we established a composite PC to classify the samples, investigate rock-water interactions, and define an indicator to evaluate the potential of sea water inrush. Note that not all data sets are suitable for PCA. First, Bartlett's test of sphericity should be used to examine the hypothesis that the variables are uncorrelated in the data set. Second, the Kaiser–Meyer–Olkin (KMO) measure of sampling adequacy should be performed to check the appropriateness of PCA. A high KMO value (between 0.5 and 1.0) indicates that PCA is appropriate, while values below 0.5 imply that PCA may not be appropriate (Jolliffe 2002).

## Results

### Site Survey Results

Over 5000 rock joints were measured in the mine area and nearly all were smooth and flat (indicating that they were shear fissures). Figure 4a, b illustrate the strike direction of joints in the hanging wall and footwall of F1, respectively. The prevailing direction of rock joints in this mine area is slightly different from that in the footwall. Furthermore, the prevailing strike direction of rock joints is northwest for the alteration zone (Fig. 4d) and northeast for the rock surrounding the alteration (Fig. 4c). Nineteen typical water samples were collected from the −105 m sublevel and 13 samples from the −135 m sublevel (Fig. 5). In addition, 13 surface water samples were collected from the Bohai Sea, Wang River, fish ponds, precipitation and local residents' drinking wells.

### Conservative Ion Test Results

The test results (Fig. 6 and supplemental Table 1) indicated that the samples were geochemically quite different. The mineralization and water quality type of the Wang river water, precipitation, and seawater were: 1.0 g/L of Cl–Ca·Na (Wang River water); 0.1 g/L of $HCO_3$-Na·Ca (precipitation); 29.4 to approximately 30.0 g/L of Cl–Na (seawater). In addition, the mineralization of Quaternary groundwater and mine water ranged from 0.4 to 38.4 g/L and from 37.2 to 82.6 g/L, respectively, which was generally higher than that of the overlying Bohai seawater. Obviously, the mine water contains brine water. The $K^+$ concentration in most of the mine water samples (0.132–0.295 g/L) was much less than in the sea water (0.35–0.365 g/L), presumably showing that the rock can adsorb $K^+$ from the water. The $Cl^-$ correlated well with $SO_4^{2-}$, $Na^+$ and $Mg^{2+}$, so the latter three variables could be omitted. The $CO_2$ and $HCO_3^-$ were also omitted due to their very low concentrations and chemical instability. Then, $Cl^-$, $K^+$, $Ca^{2+}$, $\gamma SO_4^{2-}/\gamma Cl^-$ and $\gamma Na^+/\gamma Cl^-$ were selected as HCA variables, and the HCA produced a dendrogram (supplemental Fig. 3). The $\gamma SO_4^{2-}/\gamma Cl^-$ and $\gamma Na^+/\gamma Cl^-$ were environmental indices (Li et al. 2014a, b; Ma et al. 2007). The correlation between the variables is shown in Table 1.

The HCA indicated that in the Xinli mine area, pore water in the Quaternary unconsolidated aquifer, samples 01, 08, 09, 05, 03, 02, 10, 06, 04 in the −105 m sublevel, and 06, 07, and 08 in the −135 m sublevel were chemically

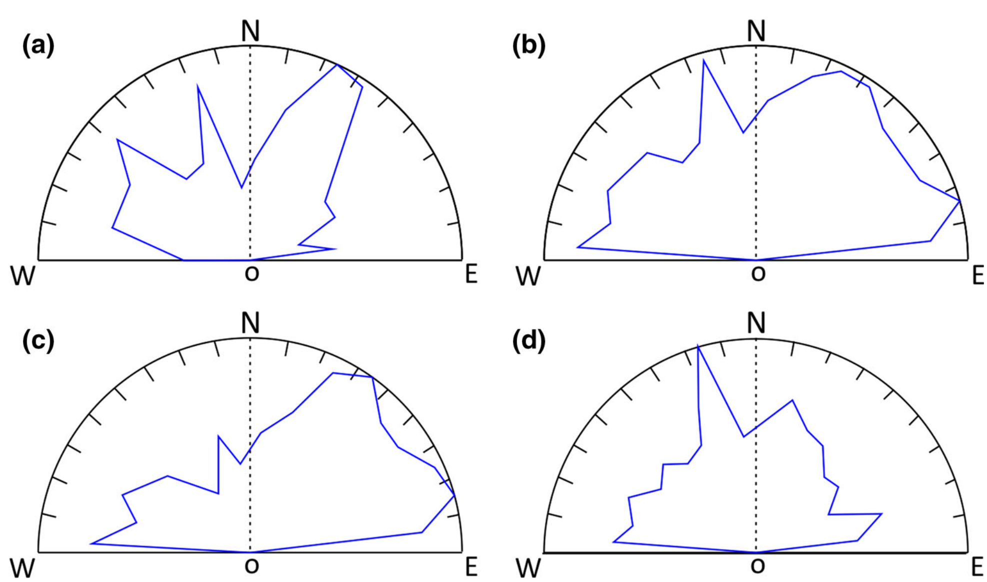


**Fig. 4** Strike rose diagram of joints in the: **a** hanging wall, **b** footwall, **c** rock surrounding the alteration zone in the footwall, and **d** alteration zone in the footwall

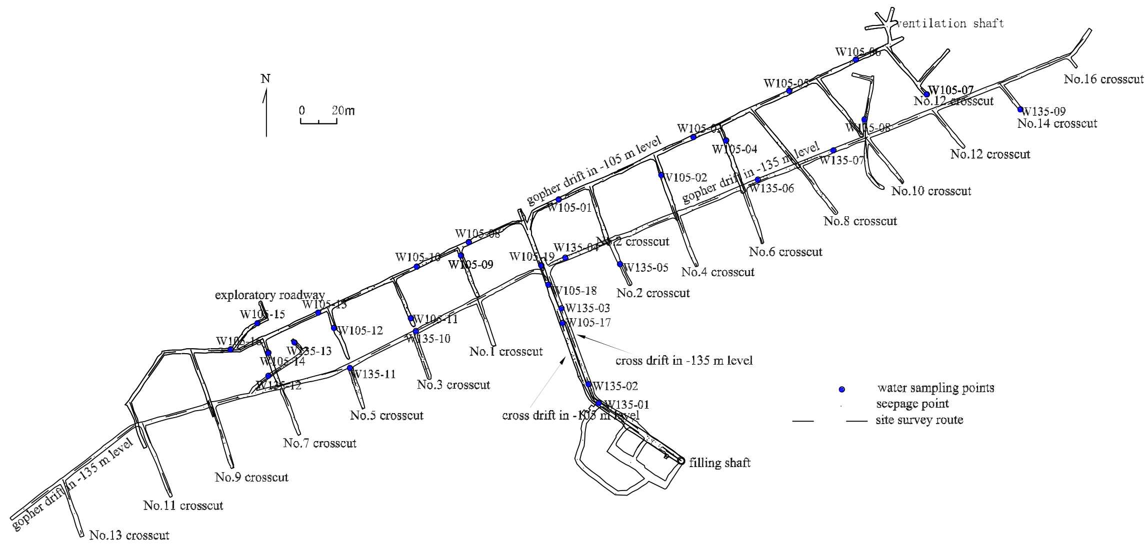


**Fig. 5** Hydrochemical survey and sampling

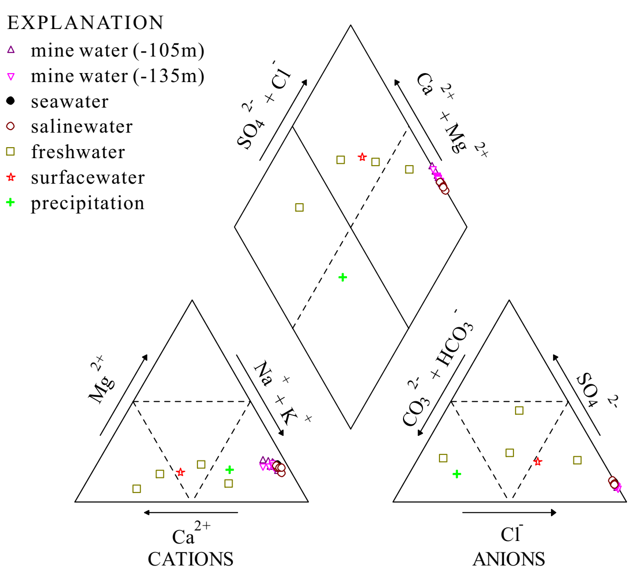


**Fig. 6** Piper diagram for the water samples

close to sea water (Figs. 5, 6, and supplemental Fig. 3). In the −105 m sublevel, the samples that were chemically close to sea water were from the northeastern gopher drift in the footwall of F1. Sample W105-07, from the No. 12 crosscut, was quite different from sea water, with very high mineralization. In the -135 m sublevel, the samples that were similar to sea water were from the northeastern gopher drift between the no. 6 and no. 9 crosscut in the F1 footwall. W135-09, located in the No. 14 crosscut, was from seepage from the hanging wall and was chemically quite different from sea water.

In the PCA, we carried out a Bartlett's sphericity test and got a value of 728.011 for the Bartlett Chi square statistic (for 21° of freedom and a minimum significance level of 0), which confirmed that the original variables were not orthogonal, but correlated. Additionally, the measure of sampling adequacy (MSA) obtained by the Kaiser–Meyer–Olkin method (KMO) was 0.802, indicating a good MSA for PCA.

PCA transformed seven variables into two PCs (Table 2). The PC score of each sample equals the product of the loadings of the seven chemical variables on the PCs, and the standardized values of these variables. To classify these samples, we defined a composite principal component (CPC) score (Eq. 2):

**Table 1** Correlation matrix of hydrochemical variables of water samples

| Correlation coefficient | $HCO_3^-$ | $Cl^-$ | $SO4^{2-}$ | $K^+$ | $Na^+$ | $Ca^{2+}$ | $Mg^{2+}$ |
|---|---|---|---|---|---|---|---|
| $HCO_3^-$ | 1.000 | | | | | | |
| $Cl^-$ | 0.572 | 1.000 | | | | | |
| $SO_4^{2-}$ | 0.608 | 0.986 | 1.000 | | | | |
| $K^+$ | 0.295 | 0.603 | 0.679 | 1.000 | | | |
| $Na^+$ | 0.602 | 0.996 | 0.991 | 0.630 | 1.000 | | |
| $Ca^{2+}$ | 0.391 | 0.888 | 0.823 | 0.301 | 0.854 | 1.000 | |
| $Mg^{2+}$ | 0.510 | 0.990 | 0.971 | 0.574 | 0.981 | 0.910 | 1.000 |

**Table 2** Loadings of 7 chemical variables on principal components (PC)

| Variable | PC1 | PC2 |
|---|---|---|
| $HCO_3^-$ | 0.266646 | −0.13627 |
| $Cl^-$ | 0.424443 | −0.05942 |
| $SO_4^{2-}$ | 0.423787 | 0.06706 |
| $K^+$ | 0.276826 | 0.876002 |
| $Na^+$ | 0.42462 | −0.01107 |
| $Ca^{2+}$ | 0.369617 | −0.44316 |
| $Mg^{2+}$ | 0.419102 | −0.0975 |
| Eigenvalue | 5.485 | 0.741 |
| % Variance explained | 78.361 | 10.586 |
| % Cumulative variance | 78.361 | 88.946 |

$$\text{CPC score} = \text{PC1 score} \times \text{PC1 Variance explained } (\%) + \text{PC2 score} \times \text{PC2 Variance explained } (\%) \quad (2)$$

The PC scores and the CPC scores of all samples are shown in supplemental Table 2. We classify the samples into five groups in terms of the CPC score (supplemental Table 3). Fresh water samples belong to one group with a CPC score ranging from −4.33165 to −1.002. The rest of the samples were evenly divided into four groups with CPC scores ranging from −1.0021 to 3.0369. The $Cl^-$, $Mg^{2+}$, $Na^+$ and $SO_4^{2-}$ show a significant positive linear correlation with each other (Table 1) and had similar loadings on PC1, while $K^+$ has a big loading on PC2 (Table 2).

PCA indicates that, in the Xinli mine area, groundwater in the Quaternary unconsolidated aquifer, samples 01, 08, 05, 09, 03, 04, 02 in the −105 m sublevel, and 07, 06, 08, 05 in the −135 m sublevel were chemically similar to sea water. Overall, the mine waters chemically similar to seawater were located above the mined out area.

## Discussion

### Mine Water Sources

Many factors, such as the dissolution by meteoric water, evaporation-concentration, desulfurization, cation exchange and adsorption, and mixing, affect the groundwater geochemistry in this mine area. The brine groundwater in the Xinli Mine resulted from evaporation-concentration of paleo-seawater and desulfurization (Ma et al. 2007). Evaporation and concentration effects increase ion concentrations and can even produce gypsum. Desulfurization refers to the reduction of $SO_4^{2-}$ to $H_2S$, which is a common phenomenon in anoxic groundwater.

The formation of the gold deposit in the Xinli Mine involved sericitization (Eq. 3), which increases $K^+$ concentrations, and potash feldspathization (Eq. 4), which decreases $K^+$ concentrations (Sun et al. 2002).

$$3KAlSi_3O_8(\text{potassium feldspar}) + H_2O \rightarrow KAl_2(AlSi_3O_{10})(OH)_2(\text{sericte}) + 6SiO_2 + K_2O \quad (3)$$

$$6[NaAlSi_3O_8(\text{albite}) + CaAl_2Si_2O_8(\text{anorthite})] + 5K_2O \rightarrow 10KAlSi_3O_8(\text{potassium feldspar}) + 6CaO + 3Na_2O + 4Al_2O_3 \quad (4)$$

Groundwater tends to exchange ionic constituents with rock and soil. Cation exchange depends on both the pH of the solution and the ion characteristics. The higher the valence of the cations, the greater its affinity to rock. For cations of the same valence, affinity generally increases with the atomic number and the ionic radius. The normal order of affinity to rock/soil is $Ca^{2+} > Mg^{2+} > K^+ > Na^+$. Therefore, cation exchange and adsorption normally decrease $Ca^{2+}$, $Mg^{2+}$, and $K^+$ concentrations and increase $Na^+$ concentrations. From supplemental Table 1, we can see that the $K^+$ concentration is much higher in seawater than in mine water, which may indicate the effects of potash feldspathization and cation exchange.

The PCA results show that there are significant positive linear correlations among $Cl^-$, $Mg^{2+}$, $Na^+$, and $SO_4^{2-}$ and that these four conservative ions have similar loadings on PC1, while $K^+$ has a large loading on PC2. Considering the various water–rock interaction, we inferred that PC1 reflects the concentration effect and PC2 reflects the effects of potash feldspathization and cation exchange. We could thus use the CPC (Eq. 2) as an indicator to assess the risk of a sea water inrush, or simply use $K^+$ and $Na^+$ concentrations to assess the mine water sources.

### Seepage Channels

Large-scale underground excavation is bound to induce stress field variations in the surrounding rock mass, which can cause rock deformation, movement, and even failure, thereby influencing permeability. The transmissibility coefficient of rock mass is proportional to the cube of the equivalent aperture (Singhal and Gupta 2010).

$$T = kA = \frac{wh_e^3}{12} \quad (5)$$

where $T$ is the transmissibility coefficient, $k$ is intrinsic permeability, $A$ is the cross-sectional area, $h_e$ is the equivalent aperture, and $w$ the width of the cross-section. Thus,

$$k = \frac{h_e^2}{12} \quad (6)$$

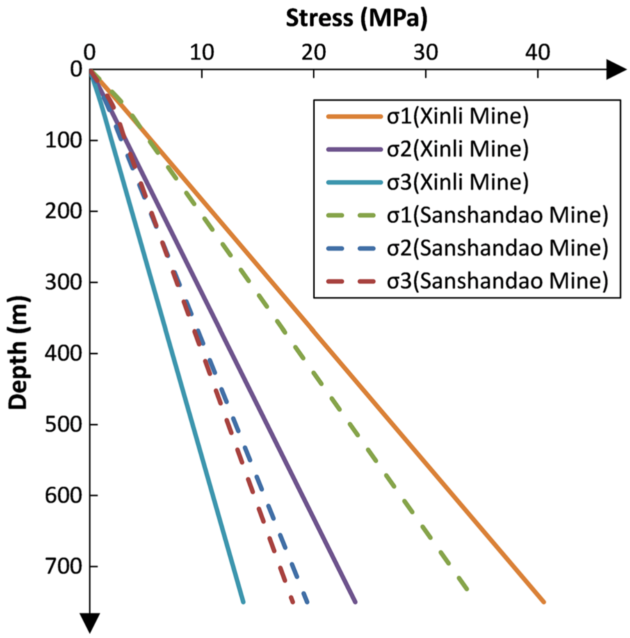


**Fig. 7** Principal stresses in Xinli Mine and Sanshandao Mine

For laminar flow, we can use Darcy's law to describe the volumetric flow rate, *Q*, as follows.

$$Q = VA \tag{7}$$

where *V* is Darcy velocity. If *K* is the hydraulic conductivity, $\eta$ is the dynamic viscosity of water, $\rho$ is the density of the fluid, and $\frac{dh}{dl}$ is the hydraulic gradient, then the governing equations are:

$$V = -K\frac{dh}{dl} \tag{8}$$

$$K = k\rho g/\eta \tag{9}$$

$$Q = -\frac{\rho g w h_e^3}{12\eta}\frac{dh}{dl} \tag{10}$$

Fluid flow in fractures is greatly influenced by the effective stress, which is taken to be the normal stress on the fracture minus the fluid pressure. Positive effective stress reduces fracture aperture and thereby reduces the permeability of fractured rocks. Stress is a directional phenomenon and determines the permeability of different fracture sets in a rock mass. Fractures parallel to the maximum principal stress tend to be widened and fractures perpendicular to the maximum principal stress tend to be narrowed.

According to the current far-field stress regime in the Xinli Mine area (Liu et al. 2012) and in the adjacent Sanshandao Mine area (Miao et al. 2004), the maximum principal stress ($\sigma_1$) strikes northwest, the minimum principal stress ($\sigma_3$) strikes northeast, and the orientation of the intermediate principal stress ($\sigma_2$) is vertical (Fig. 7). All of the faults and joints in the Xinli Mine area are shear fractures. The prevailing strike direction of joints in the alteration zone of footwall is northwest, parallel to $\sigma_1$. Thus, the northwest-striking joints in the alteration zone are potential seepage channels. Figure 8 shows the basic fault types and the associated principal stress orientations (Singhal and Gupta 2010). $F_2$ is a typical steep strike-slip fault and $F_1$ is a reverse fault. The plane of $F_2$, which is similar to the $F_3$ plane in the Sanshandao Mine area, is parallel to the maximum principal stress direction and tends to widen. The $F_1$ plane is perpendicular to the maximum principal stress and tends to narrow. Therefore, $F_2$ is also a potential channel for groundwater inflow.

## Conclusions

A hydrochemical method of predicting the inflow of sea water into an undersea mine was proposed. We used water quality analysis reinforced by multivariate statistical

**Fig. 8** Main fault types and the associated principal stress orientations according to Anderson's (1951) theory of faulting: **a** normal, **b** reverse (or thrust), and **c** strike-slip

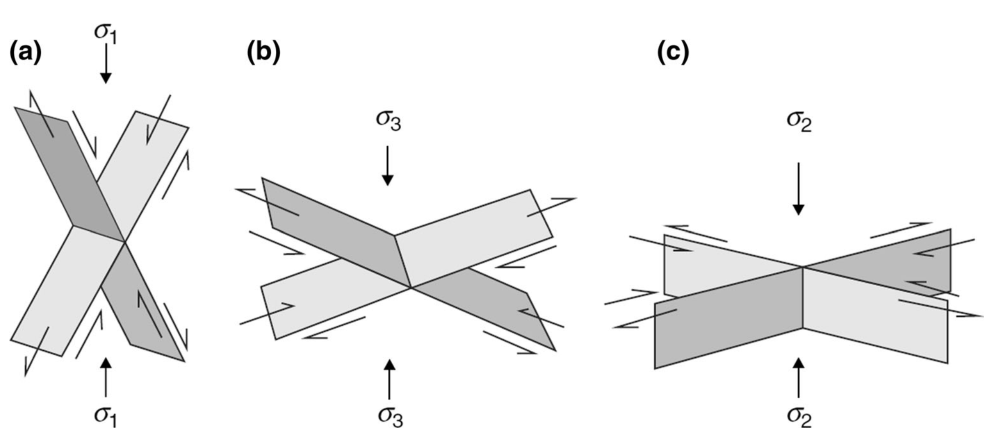

analysis to recognize the mine water sources. Using this approach, the occurrence of catastrophic sea water inflow in Xinli Mine was predicted. For the upward-filling mining in Xinli Mine, the potential water inrush channels are located in the hanging wall of $F_1$. A CPC was proposed as an indicator of the risk of seawater inrush into the mine. This indicator can be calculated from the concentrations of $Na^+$, $Cl^-$, $Mg^{2+}$, $SO_4{}^{2-}$ and $K^+$ and reflects the effects of concentration, potash feldspathization, and cation exchange. Mine water flow, water quality monitoring, and land surface displacement measurements are essential to ensure safe production at the Xinli Mine.

**Acknowledgments** This study was financially supported by the Natural Science Foundation of the Hubei Province of China (Grant 2014CFB169), Shanxi Provincial Basic Research Program—Coal Bed Methane Joint Research Foundation (Grants 2015012014 and 2014012001), the National Science and Technology Major Project of the Ministry of Science and Technology of China During "13th Five-Year Plan" (Grants 2016ZX05067001-006, 2016ZX05067001-007 and 2016ZX05043001-001), the Fundamental Research Foundation for the National University (China University of Geosciences—Wuhan, Grant CUGL120258), the National Natural Science Foundation of China (Grant 41172145), and the China Scholarship Council. The authors thank the editors and anonymous reviewers.

## References


Güler C, Kurt MA, Alpaslan M, Akbulut C (2012) Assessment of the impact of anthropogenic activities on the groundwater hydrology and chemistry in Tarsus coastal plain (Mersin, SE Turkey) using fuzzy clustering, multivariate statistics and GIS techniques. J Hydrol 414–415:435–451

Guo DF (2004) Principal component analysis on the ions in the groundwater intrusion area of Laizhou Bay. Mar Sci 28(9):6–9 **(In Chinese)**

Jolliffe IT (2002) Principal component analysis. Springer, New York

Kurchikov AR, Plavnik AG (2009) Clustering of groundwater chemistry data with implications for reservoir appraisal in West Siberia. Russ Geol Geophys 50:943–949

Li X, Wang SJ, Liu TY, Ma FS (2004) Engineering geology, ground surface movement and fissures induced by underground mining in the Jinchuan Nickel Mine. Eng Geol 76(1–2):93–107

Li GQ, Ma FS, Meng ZP (2012) Analysis of connectivity between an undersea metal mine and overlying seawater in Xinli mine. J Central South Univ 43(10):3938–3945 **(In Chinese)**

Li GQ, Wang XQ, Meng ZP, Zhao HJ (2014a) Seawater inrush assessment based on hydrochemical analysis enhanced by hierarchy clustering in an undersea goldmine pit, China. Environ Earth Sci 71(12):4977–4987. doi:10.1007/s12665-013-2888-8

Li GQ, Wang XQ, Yin GM (2014b) Application of principal component analysis in identifying the seepage of seawater into Xinli mine pit. Chin J Geol Hazard Control 25(3):83–88 **(In Chinese)**

Liu ZX, Dang WG, He XG (2012) Undersea safety mining of the large gold deposit in Xinli District of Sanshandao gold mine. Int J Miner Metall Mater 19(7):574–583

Ma F, Yang YS, Yuan R, Cai Z, Pan S (2007) Study of shallow groundwater quality evolution under saline intrusion with environmental isotopes and geochemistry. Environ Geol 51(6):1009–1017

Ma FS, Deng QH, Cunningham D, Yuan RM, Zhao HJ (2013) Vertical shaft collapse at the Jinchuan Nickel Mine, Gansu Province, China: analysis of contributing factors and causal mechanisms. Environ Earth Sci 69:21–28. doi:10.1007/s12665-012-1930-6

Meng ZP, Li GQ, Xie XT (2012) A geological assessment method of floor water inrush risk and its application. Eng Geol 143–144:51–60. doi:10.1016/j.enggeo.2012.06.004

Miao SJ, Wan LH, Lai XP (2004) Relation analysis between in situ stress field and geological tectonism in Sanshandao gold mine. Chin J Rock Mech Eng 23(23):3396–3399

Mondal NC, Singh VS, Saxena VK, Singh VP (2011) Assessment of seawater impact using major hydrochemical ions: a case study from Sadras, Tamilnadu, India. Environ Monit Assess 177:315–335. doi:10.1007/s10661-010-1636-8

Moujabber MEL, Samra BB, Darwish T, Atallah T (2006) Comparison of different indicators for groundwater contamination by seawater intrusion on the Lebanese coast. Water Resour Manag 20:161–180. doi:10.1007/s11269-006-7376-4

Salem SBH, Moussa AB, Chkir N (2011) Geochemical and isotopic investigation of groundwater mineralization process in the Zeroud basin, central Tunisia. Carbonates Evaporites 26:301–315. doi:10.1007/s13146-011-0058-1

Seki Y, Dickson FW, Liou JG, Oki Y, Sakai H, Hirano T (1986) Geochemical prediction of impending catastrophic inflow of seawater during construction of the undersea part of the Seikan Tunnel, Japan. Appl Geochem 1(3):317–333

Singhal BBS, Gupta RP (2010) Applied hydrogeology of fractured rocks, 2nd edn. Springer, New York

Sun ZF, Zhu ZQ, Li W (2002) Geological exploration report of Xinli gold mine. Laizhou Geological and Mineral Exploration Institute, Laizhou **(In Chinese)**

Wu Q, Liu YZ, Liu DH, Zhou WF (2011) Prediction of floor water Inrush: the application of GIS-Based AHP vulnerable index method to Donghuantuo coal mine, China. Rock Mech Rock Eng 44(5):591–600

Xu XH, Wang J (1991) Prediction of coal mining water inrush. Geology Publishing House, Beijing **(In Chinese)**

Zhao HJ, Ma FS, Li GQ, Zhang YM, Guo J (2012a) Study of the hydrogeological characteristics and permeability of the Xinli Seabed Gold Mine in Laizhou Bay, Jiaodong Peninsula, China. Environ Earth Sci 65:2003–2014. doi:10.1007/s12665-011-1181-y

Zhao HJ, Ma FS, Xu JM, Guo J (2012b) In situ stress field inversion and its application in mining-induced rock mass movement. Int J Rock Mech Min Sci 53:120–128

Zhao HJ, Ma FS, Zhang YM, Guo J (2013) Monitoring and analysis of the mining-induced ground movement in the Longshou Mine, China. Rock Mech Rock Eng 46(1):207–211

Zimmerman RW (2000) Coupling in poroelasticity and thermoelasticity. Int J Rock Mech Min 37:79–87

Zimmerman RW, Bodvarsson GS (1996) Hydraulic conductivity of rock fractures. Transp Porous Med 23:1–30